PROCEEDINGS OF SCIENCE

Status of the RICOCHET experiment at the ILL

Louis Bailly-Salins[a,*] **on behalf of the RICOCHET Collaboration**

[a] *Université Grenoble Alpes, CNRS, Grenoble INP, LPSC-IN2P3, 38000 Grenoble, France*

E-mail: baillysalins@lpsc.in2p3.fr

The RICOCHET experiment aims to measure the coherent elastic neutrino-nucleus scattering induced by the antineutrinos produced by the research nuclear reactor of the Institut Laue-Langevin (ILL) in Grenoble, France. The RICOCHET Collaboration uses an array of 42-g germanium cryogenic calorimeters capable of reading out both ionization and phonon signals. Two types of calorimeters (planar and FID) are employed, which differ by their electrode design. In this contribution, the RICOCHET experiment and the performance achieved during its first commissioning phases are presented. The baseline energy resolution and the rate of background nuclear recoils (NR) between 2 and 7 keV are reported for planar detectors. The NR rate induced by cosmogenic muons is measured using events in coincidence with the muon veto with the reactor OFF and is shown to be consistent with the GEANT4 simulations. For events in anti-coincidence with the muon veto, as the sensitivity of the measurement is limited by the contamination from surface events, only upper limits are reported both with the reactor ON and OFF. The latest part of this contribution focuses on preliminary results obtained during the following commissioning phase with the first FID detectors operated in RICOCHET. These detectors offer the capability to identify surface events, and comparison with the event distributions for planar detectors suggests an improved sensitivity of FID detectors to nuclear recoils with respect to planar detectors.

The European Physical Society Conference on High Energy Physics (EPS-HEP2025)
7-11 July 2025
Marseille, France

*Speaker

 ISSN 1824-8039 . Published by SISSA Medialab.

PoS(EPS-HEP2025)150

1. Introduction

Coherent elastic neutrino-nucleus scattering (CENNS) is a neutral current neutrino interaction process through which the neutrino interacts coherently with the nucleus as a whole. CENNS was proposed by Freedman in 1974 [1], and it was observed for the first time by the COHERENT Collaboration at the spallation neutron source (SNS) of Oak Ridge National Laboratory in 2017 [2]. The measurement of CENNS offers a new probe for physics beyond the standard model (BSM) in the neutrino sector. The nuclear recoil energy spectrum at low momentum transfer is expected to be sensitive to multiple BSM scenarios [3–7], including: anomalies in the neutrino magnetic moment, non-standard interaction between neutrinos and quarks, coupling of neutrinos to new massive scalar and vector mediators, and oscillations with sterile neutrinos.

Research nuclear reactors can offer an antineutrino flux which is four orders of magnitude larger than the SNS [8, 9]. This increase in statistics should allow for a precision measurement of CENNS, opening the door to searches for BSM physics. There is an active global effort to observe CENNS from reactor antineutrinos [10–13]. The challenge in measuring reactor antineutrino-induced CENNS lies in the low energy threshold ($\sim$100 eV) needed to reach significant CENNS statistics and to probe the region of the spectrum sensitive to BSM scenarios [3].

The RICOCHET experiment [14] aims at measuring CENNS at the research nuclear reactor of the Institut Laue-Langevin (ILL) in Grenoble using an array of eighteen 42-gram germanium cryogenic calorimeters. Two types of calorimeters, described in Section 2.2, are tested: planar, and fully inter-digitized (FID) detectors [15]. This contribution summarizes the results from the initial commissioning of RICOCHET at the ILL using planar detectors (more details in [16]) and shows a comparison with preliminary results from a second phase of the commissioning employing FID detectors for the first time at the ILL.

2. Experimental setup of RICOCHET at the ILL

2.1 Experimental setup

The detectors of RICOCHET are located 8.8 m away from the core of the ILL reactor, which has a nominal thermal power of 58 MW. Multiple strategies are employed to mitigate the levels of background from radiogenic (natural radioactivity of the materials surrounding the detectors), reactogenic (neutrons, capture γ and decays of activated isotopes from the reactor and the neighbouring experiments) and cosmogenic (cosmic ray-induced particles) origin. First, the reactor building and the transfer channel (a concrete channel filled with water) on top of the experiment site provide an overburden of $\approx$ 15 m water equivalent, reducing the cosmogenic background. Also, a 22-ton external shield composed of borated high-density polyethylene (HDPE) and lead surrounds the cryostat [14]. A layer of soft iron encloses the external shield to attenuate the magnetic field generated by the surrounding experiments. Inside the cryostat, an additional, internal shielding comprising additional layers of HDPE and lead covers the cylindrical space above the detectors, as the external shielding does not cover the top of the cryostat. Additionally, an active muon veto installed around the external shielding is operated to detect cosmogenic muons, allowing us to tag coincident events in the cryogenic detectors. The muon veto is composed of 34 plastic scintillator panels ($200 \times 50 \times 3$ cm^3) arranged in 17 pairs. Pairing the panels in couples allows us to reject

single-panel triggers from the reactogenic γ background events. Six pairs of panels are placed on top of the external shielding and 11 pairs around it.

The reactor at the ILL is operated through an alternation of 'ON' of 'OFF' cycles (typically three cycles per year, with an ON period of about 50 days each). Comparing the data obtained in reactor ON and reactor OFF periods will allow us to subtract the contributions of non-reactogenic backgrounds. The neutron background at the RICOCHET site has been characterized in a previous study [14]. From this result, a signal over background ratio around unity can be expected for the CENNS measurement. The gamma background contribution is estimated in another contribution presented at this conference [17].

2.2 Cryogenic detectors

RICOCHET uses an array of germanium cryogenic calorimeters called the CryoCube, hosted in a dry-dilution ^{3}He/^{4}He cryostat. The CryoCube is composed of 18 germanium detectors disposed over two floors. Each floor contains three modules (mini-CryoCube) of three detectors each [18]. Each cryogenic calorimeter's target consists of a cylindrical 42 g germanium crystal. A key feature of the RICOCHET calorimeters is the double readout of ionization and phonon signals, which allows us to distinguish different types of interactions (electronic recoils, nuclear recoils and non-ionizing events [19, 20]). When a particle such as a neutrino scatters off a nucleus or an electron in the germanium target, the recoil of the interacting particle produces both an ionization signal through the creation of electron-hole pairs, and a phonon signal. The ionization signal is measured with aluminium electrodes deposited on the top and bottom surfaces of the germanium crystal. A polarization of $\pm 2V$ applied to the electrodes amplifies the phonon signal via the creation of secondary phonons generated by the moving charges thanks to the Neganov-Trofimov-Luke (NTL) effect [21, 22], so that the measured phonon energy E_{ph} (expressed in $\mathrm{eV_{ph}}$) is the sum of the initial recoil energy E_r and the NTL phonon contribution E_{NTL}:

$$E_{ph} = E_r + E_{NTL} = E_r + E_r Q \frac{q\,V}{\epsilon}\,, \tag{1}$$

where the ionization yield Q is defined as the ratio between the detected ionization energy E_{ion} (expressed in $\mathrm{eV_{ee}}$, where the *ee* subscript stands for electron equivalent) and the recoil energy deposited in the detector ($Q = \frac{E_{ion}}{E_r}$), q is the electron charge, V the voltage bias applied across the electrodes, and ϵ the energy required to create one electron-hole pair (around 3 eV in germanium cryogenic crystals [23]). The phonon signal is read out with a germanium neutron-transmutation-doped (Ge-NTD) thermistor biased with a current of 0.5 nA. The ionization and phonon channels are calibrated using the peak at 10.37 keV coming from the electron capture on the K shell of ^{71}Ge. The presence of this isotope results from the activation of the germanium crystals with an AmBe neutron source before deployment at the ILL. The recoil energy can be reconstructed from the measured E_{ion} and E_{ph} as:

$$E_r = E_{ph} - E_{ion} \frac{q\,V}{\epsilon}\,. \tag{2}$$

The ionization yield value depends on the type of interaction:

- electronic recoils (ER), induced by β and γ radiations, for which $Q = 1$
- nuclear recoils (NR) induce by CENNS and neutron scattering, for which $Q \simeq 0.2$ for keV-scale recoils [24–26]

- non-ionizing or heat-only events (HO), for which $Q = 0$

which allows us to perform particle identification and lower our background levels.

The RICOCHET experiment employs two types of electrode geometries for the ionization readout: planar and fully inter-digitized (FID). Figure 1 shows a vertical section of the two detector types to visualize the two electrode geometries. The planar detectors (Fig. 1, left) have two electrodes, one at the top and one at the bottom. The FID detectors (Fig. 1, right) have four circular concentric electrodes grouped in two pairs: A-C, called the veto electrodes, and B-D, the fiducial electrodes. In standard configuration, the fiducial electrodes (B / D) are polarized at (+2 / -2 V) and the veto electrodes (A / C) are biased at (-0.5 / 0.5 V) such that recoils happening in the bulk of the crystal induce signals only on the fiducial electrodes while recoils happening near the surface (first few millimeters) induce a signal on the veto electrodes. This means that, contrary to planar detectors, FID detectors offer the capability to identify surface events (see Section 3), but this comes at the cost of a reduced fiducial volume with respect to planar detectors.

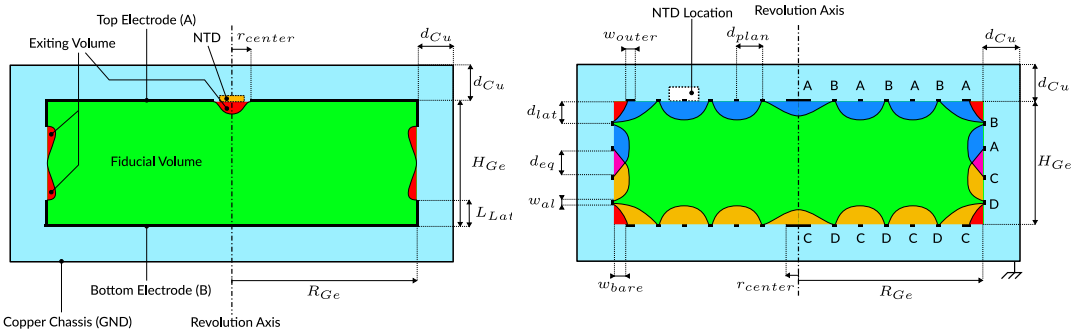

Figure 1: Schematics of the planar (left) and FID (right) detector designs, shown within their copper holder — the electrically grounded rectangle separated from the germanium target by vacuum (shown in light blue). The different charge collection zones are depicted: the fiducial volume is shown in green and, for the FID, the top and bottom veto volumes are shown in blue and orange, respectively. Reproduced from [27].

3. Commissioning results

The commissioning of RICOCHET at the ILL happened in a staged way. It started in February 2024 with the validation of the cryogenics performance through a week-long run with no detectors in the cryostat. A base temperature of 8.6 mK was achieved. The first mini-CryoCube module, composed of three planar detectors, was then operated during two commissioning runs: RUN013 lasted from February to April 2024, and RUN014 from May to October 2024. The calorimeters were operated at temperatures ranging from 12.0 mK to 15.6 mK. One of the ionization channels of one calorimeter was not operational, so the data taking focused on the other two detectors (named RED167 and RED237).

Due to the location of the experiment above pumps used to operate the reactor, additional vibrations can reach the detectors in reactor ON periods, degrading their energy resolution. RUN013 tested the detector performance during a reactor ON period for the first time, with the main objective

of mitigating the effect of vibrations. In RUN014, the inner shielding and the outer muon veto were installed, which provided us with the perfect opportunity to measure the onsite backgrounds with one mini-CryoCube. A laser diode, illuminating the detectors through optical fibers, was also installed before RUN014. It is used for detector characterization purposes and to periodically neutralize the space charge accumulating in the germanium crystals.

The main results from RUN013 and RUN014 are discussed in [16] for both RED167 and RED237. Section 3.1 summarizes the results achieved with planar detectors in RUN014, focusing on the RED167 detector. The payload was increased to 3 mini-CryoCubes (five planar detectors and four FID detectors) during RUN015 to stage the detector deployment. The FID detectors were operated at the ILL for the first time. This run lasted from January 2025 to June 2025. Section 3.2 presents the first results obtained by one FID detector in RUN015.

3.1 RUN014 commissioning results

The data processing of the ionization, phonon and muon veto data, as well as the data analysis strategy of this analysis, are detailed in [16]. Regarding the detector performance, baseline energy resolutions of 40 eV_{ee} and 50 to 80 eV_{ph} were obtained after setup optimization for the ionization and phonon channels, respectively. Figure 2 shows events recorded by the detector RED167 during RUN014 as a function of the measured ionization yield and recoil energy. Two data samples corresponding to different data taking periods are shown: in black, during the reactor ON period and in pink, during the period when a Cf-252 neutron source was installed to study the response of the germanium detectors to neutrons. The livetime amounts to 155 h and 253 h for the reactor ON and the Cf-252 periods, respectively. For both samples, a muon veto anti-coincidence selection was applied. Multiple populations of events, already introduced earlier, appear: electronic recoils ($Q = 1$), nuclear recoils induced by neutrons ($Q \simeq 0.2$) and heat-only events ($Q = 0$). In addition, a fourth population of events is present, spread uniformly in ionization yield between 0 and 1. They are believed to correspond to events happening near the surface of the germanium crystals, which suffer from incomplete charge collection. Such surface events can originate from β decays on the surface of the detector or its copper holder, or from electrons produced through photoelectric or Compton interactions in the copper holder.

The detection of CENNS requires low backgrounds that are achieved in RICOCHET through passive shielding and active muon veto (Sec. 2.1) and particle identification (Sec. 2.2). Following the installation of the inner shielding and outer muon veto, RUN014 was the first occasion to measure the on-site experimental backgrounds during both reactor ON and reactor OFF periods and compare them with the simulations. The rates were calculated between 2 and 7 keV*. For this analysis, the measured event rates are corrected using the combined efficiency of the trigger algorithm, reconstruction algorithm, and data selection. This efficiency was measured, using the laser diode, as the ratio of reconstructed laser-induced events passing the data selection to the known number of injected laser pulses [16]. Due to the presence of the surface events contamination evidenced in Figure 2, the NR rate cannot be obtained directly from counting the events in the expected NR band position. Instead, a likelihood analysis was performed to distinguish NR events

*This range excludes CENNS events from the reactor ON data below 2 keV, events from the ^{71}Ge L-shell line at 1.3 keV and the Cu fluorescence line at 8.1 keV.

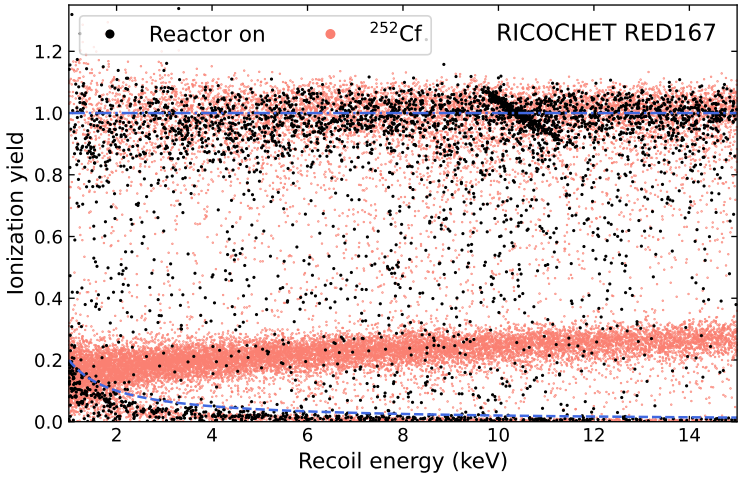

Figure 2: Ionization yield as a function of the recoil energy for the reactor ON data (black) superimposed to the ^{252}Cf neutron source data (pink) for the planar detector RED167. The expected position of ER events and the 0.2 keV$_{ee}$ ionization selection used to identify HO events are indicated with a blue dash-dotted and dashed line, respectively. Reproduced from [16].

from surface events, using all events with ionization yield between 0 and 0.5. The surface events background is modeled as a linear function of the ionization yield, and the distribution of NR events is modeled as a Gaussian whose mean and sigma are determined by fitting the Cf-252 data sample which offers high NR statistics. The position and resolution of the NR gaussian were fixed when fitting the ionization yield event distributions for three other samples: events in coincidence with the muon veto for the reactor OFF period, and events in anti-coincidence with the muon veto, both in reactor OFF and ON. For the coincident sample, a NR rate of 14 ± 3 events/(kg day keV) is obtained for RED167, matching very well the expected rate from the cosmogenic background GEANT4 simulations (15 ± 2 events/(kg day keV)). For the anti-coincident events, the NR rate is lower than the surface background, so only an upper limit can be set at a 90% confidence level. When considering both of the operated detectors, the combined upper limit at a 90% confidence level is 9 events/(kg day keV) (15 events/(kg day keV)) in reactor ON (reactor OFF). This is compatible with the GEANT4 simulations which yield a NR rate of 4.6 ± 0.8 events/(kg day keV) for cosmogenic background and 0.4 ± 0.1 events/(kg day keV) for reactogenic background.

3.2 Preliminary FID performance for RUN015

Estimating more precisely the background NR rate from neutrons will require to suppress the surface events background. Two strategies are explored by the RICOCHET Collaboration: etching the copper holders of planar detectors to reduce their surface backgrounds, and using FID detectors which offer the capability to reject surface events due to their electrode design. The first FID detectors operated by RICOCHET were installed for RUN015. The ionization yield as a function of the recoil energy measured by the detector FID147 during RUN015 is shown in Figure 3. Events recorded during the reactor OFF period (272 hours of livetime) and during the Cf-252 period (102 hours livetime) are shown. Here, no muon veto anticoincidence selection is applied because

the muon veto was not installed during this specific data-taking period. Compared to Figure 2, the surface events population is drastically reduced by applying a fiducial cut — a data selection to remove events with signals on the veto electrodes (see Section 2.2). After the fiducial data selection, some events (black) are clearly distinguishable in the reactor OFF sample within the NR band. Given the absence of muon veto selection, those events are likely caused by cosmogenic neutrons. Even though proper comparison with Figure 2 will require rejecting events coincident with the muon veto, this preliminary result suggests that FID detectors have an improved sensitivity to nuclear recoils compared to planar detectors. Further analysis of the RUN015 data, including the estimation of the NR rates for FID detectors using the muon veto, is ongoing. Additionally, an improved phonon resolution of 30 eV_{ph} was achieved in RUN015 for the best-working detector.

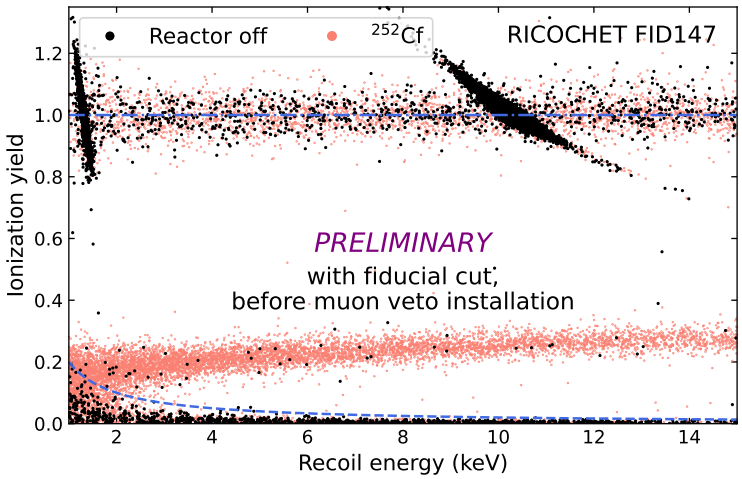

Figure 3: Ionization yield as a function of the recoil energy for the reactor OFF data (black) superimposed to the ^{252}Cf neutron source data (pink) for the detector FID147. The expected position of ER events and the selection used to identify HO events are indicated with a blue dash-dotted and dashed line, respectively.

4. Conclusion

The RICOCHET experiment has been successfully installed and commissioned at the ILL. During the first commissioning runs, baseline energy resolutions of 40 eV_{ee} for the ionization channel and 50-80 eV_{ph} for the phonon channel were achieved with planar detectors. The rate of background nuclear recoil events in coincidence with the muon veto is in agreement with the cosmogenic background simulations. For events in anticoincidence with the muon veto, a combined upper limit of 9 events/(kg day keV) at a 90% confidence level has been obtained for the reactor ON period. The sensitivity of this analysis was found to be limited by the surface event background. However, during the following commissionning run (RUN015), additional cryogenic calorimeters were deployed, including FID detectors which offer surface event rejection capabilities thanks to their different electrode design. Further analysis of RUN015 data is in progress. Finally, the first science run with the full payload of 18 germanium calorimeters (including 11 FID detectors and four planar detectors with etched copper holders), amounting to a mass of 0.76 kg, started in July 2025 and is currently ongoing.

References

[1] D.Z. Freedman, *Coherent effects of a weak neutral current*, *Phys. Rev. D* **9** (1974) 1389.

[2] COHERENT Collaboration, *Observation of coherent elastic neutrino-nucleus scattering*, *Science* **357** (2017) 1123.

[3] M. Lindner, W. Rodejohann and X.-J. Xu, *Coherent neutrino-nucleus scattering and new neutrino interactions*, *J. High Energ. Phys.* **2017** (2017) 97.

[4] J. Billard, J. Johnston and B.J. Kavanagh, *Prospects for exploring New Physics in Coherent Elastic Neutrino-Nucleus Scattering*, *J. Cosmol. Astropart. Phys.* **2018** (2018) 016.

[5] M. Cadeddu, C. Giunti, K.A. Kouzakov, Y.F. Li, A.I. Studenikin and Y.Y. Zhang, *Neutrino charge radii from COHERENT elastic neutrino-nucleus scattering*, *Phys. Rev. D* **98** (2018) 113010.

[6] J. Billard, *Searching for Dark Matter and New Physics in the Neutrino Sector with Cryogenic Detectors*, accreditation to supervise research, Université Claude Bernard Lyon 1, 2021.

[7] M.A. Corona, M. Cadeddu, N. Cargioli, F. Dordei, C. Giunti and C.A. Ternes, *The Standard Model tested with neutrinos*, 2025. 10.48550/arXiv.2504.05272.

[8] COHERENT Collaboration, *Simulating the neutrino flux from the Spallation Neutron Source for the COHERENT experiment*, *Phys. Rev. D* **106** (2022) 032003.

[9] C. Augier, G. Beaulieu, V. Belov, L. Berge, J. Billard, G. Bres et al., *Ricochet Progress and Status.*, *J. Low Temp. Phys.* **212** (2023) 127.

[10] J. Colaresi, J.I. Collar, T.W. Hossbach, A.R.L. Kavner, C.M. Lewis, A.E. Robinson et al., *First results from a search for coherent elastic neutrino-nucleus scattering at a reactor site*, *Phys. Rev. D* **104** (2021) 072003.

[11] N. Ackermann, H. Bonet, A. Bonhomme, C. Buck, K. Fülber, J. Hakenmüller et al., *Direct observation of coherent elastic antineutrino–nucleus scattering*, *Nature* **643** (2025) 1229.

[12] NUCLEUS Collaboration, *Commissioning of the NUCLEUS Experiment at the Technical University of Munich*, *Phys. Rev. D* **112** (2025) 072013 [2508.02488].

[13] MINER Collaboration, D. Mondal, W. Baker, M. Chaudhuri, J.B. Dent, R. Dey, B. Dutta et al., *CEvNS Search with Cryogenic Sapphire Detectors at MINER: Results from the TRIGA reactor data and Future Sensitivity at HFIR*, 2025. 10.48550/arXiv.2510.15999.

[14] RICOCHET Collaboration, *Fast neutron background characterization of the future Ricochet experiment at the ILL research nuclear reactor*, *Eur. Phys. J. C* **83** (2023) 20.

[15] EDELWEISS Collaboration, *Performance of the EDELWEISS-III experiment for direct dark matter searches*, *J. Inst.* **12** (2017) P08010.

[16] RICOCHET Collaboration, A. Armatol, C. Augier, L. Bailly-Salins, G. Baulieu, L. Bergé, J. Billard et al., *Characterization of mini-CryoCube detectors from the Ricochet experiment commissioning at the Institut Laue-Langevin*, 2025. 10.48550/arXiv.2507.22751.

[17] RICOCHET Collaboration, *Gamma background model for the Ricochet Experiment*, in *PoS(EPS-HEP2025)*, vol. 485, p. 189, SISSA Medialab (2025).

[18] RICOCHET Collaboration, *First demonstration of 30 eVee ionization energy resolution with Ricochet germanium cryogenic bolometers*, *Eur. Phys. J. C* **84** (2024) 186.

[19] P. Adari, A.A. Aguilar-Arevalo, D. Amidei, G. Angloher, E. Armengaud, C. Augier et al., *EXCESS workshop: Descriptions of rising low-energy spectra*, *SciPost Phys. Proc.* **9** (2022) 001.

[20] D. Baxter, R. Essig, Y. Hochberg, M. Kaznacheeva, B. von Krosigk, F. Reindl et al., *Low-Energy Backgrounds in Solid-State Phonon and Charge Detectors*, *Annu. Rev. Nucl. Sci.* **75** (2025) 301.

[21] B.S. Neganov and V.N. Trofimov, *Colorimetric method measuring ionizing radiation*, *Otkryt. Izobret.* **146** (1985) 215.

[22] P.N. Luke, *Voltage-assisted calorimetric ionization detector*, *J. Appl. Phys.* **64** (1988) 6858.

[23] M.P. Chapellier, G. Chardin, L. Miramonti and X.F. Navick, *Physical interpretation of the Neganov–Luke and related effects*, *Physica B: Condens. Matter* **284–288** (2000) 2135.

[24] K.W. Jones and H.W. Kraner, *Stopping of 1- to 1.8-keV ^{73}Ge Atoms in Germanium*, *Phys. Rev. C* **4** (1971) 125.

[25] K.W. Jones and H.W. Kraner, *Energy lost to ionization by 254-eV ^{73}Ge atoms stopping in Ge*, *Phys. Rev. A* **11** (1975) 1347.

[26] Y. Messous, B. Chambon, V. Chazal, M. De Jésus, D. Drain, C. Pastor et al., *Calibration of a Ge crystal with nuclear recoils for the development of a dark matter detector*, *Astropart. Phys.* **3** (1995) 361.

[27] D. Misiak, *Développements de Nouveaux Détecteurs Cryogéniques Bas Seuils Pour La Recherche de Matière Noire Légère et La Physique Des Neutrinos de Basse Énergie*, Ph.D. thesis, Université de Lyon, 2021.

PoS(EPS-HEP2025)150

Full Authors List: The RICOCHET Collaboration

A. Armatol[a], C. Augier[a], L. Bailly-Salins[b], G. Baulieu[a], L. Bergé[c], J. Billard[a], J. Blé[b], G. Bres[d], J-.L. Bret[d], A. Broniatowski[c], M. Calvo[d], A. Cavanna[e], A. Cazes[a], E. Celi[f], D. Chaize[a], M. Chala[b], M. Chapellier[c], L. Chaplinsky[g], G. Chemin[b], R. Chen[f], J. Colas[a], L. Couraud[e], E. Cudmore[h], M. De Jesus[a], N. Dombrowski[i], L. Dumoulin[c], A. Durnez[e], O. Exshaw[d], S. Ferriol[a], E. Figueroa-Feliciano[f], J. A. Formaggio[i], S. Fuard[j], J. Gascon[a], A. Giuliani[c], C. Goy[b], C. Guerin[a], E. Guy[a], L. Haegel[a], S. A. Hertel[g], C. Hoarau[b], Z. Hong[h], J.-C. Ianigro[a], Y. Jin[e], A. Juillard[a], T. Khussainov[k †], A. Kubik[h ‡], J. Lamblin[b], H. Lattaud[a], T. Le Bellec[a], L. Leroy[e], M. Li[i], A. Lubashevskiy[k §], S. Marnieros[c], N. Martini[a], J. Minet[d], A. Monfardini[d], F. Mounier[a], V. Novati[b], E. Olivieri[c], P. K. Patel[g], E. Perbet[b], H. D. Pinckney[i], D. V. Poda[c], D. Ponomarev[k §], W. Van De Pontseele[l], J.-S. Real[b], F. C. Reyes[i], A. Rodriguez[f], M. Rousseau[b], S. Rozov[k], I. Rozova[k], B. Ryan[i], D. Sabhari[f], S. Scorza[b], R. Serra[j,b], Ye. Shevchik[k], T. Soldner[j], A. Stutz[b], Ch. Ulysse[e], L. Vagneron[a], S. Vasilyev[k], F. Vezzu[b], P. Vittaz[a], E. Yakushev[k], J. Yang[i], D. Zinatulina[k].

[a] Univ Lyon, Université Lyon 1, CNRS/IN2P3, IP2I-Lyon, F-69622, Villeurbanne, France
[b] Univ. Grenoble Alpes, CNRS, Grenoble INP, LPSC-IN2P3, 38000 Grenoble, France
[c] Université Paris-Saclay, CNRS/IN2P3, IJCLab, 91405 Orsay, France
[d] Univ. Grenoble Alpes, CNRS, Grenoble INP, Institut Néel, 38000 Grenoble, France
[e] Univ. Paris-Saclay, CNRS, C2N, Palaiseau, 91120 Palaiseau, France
[f] Department of Physics and Astronomy, Northwestern University, IL 60208, USA
[g] Department of Physics, University of Massachusetts at Amherst, Amherst, MA 01003, USA
[h] Department of Physics, University of Toronto, ON M5S 1A7, Canada
[i] Laboratory for Nuclear Science, Massachusetts Institute of Technology, Cambridge, MA 02139, USA
[j] Institut Laue-Langevin, CS 20156, 38042 Grenoble Cedex 9, France
[k] Department of Nuclear Spectroscopy and Radiochemistry, Laboratory of Nuclear Problems, JINR, Dubna, Moscow Region 141980, Russia
[l] Physics Department, Colorado School of Mines, Golden, CO 80401, USA

[†] also at: Institute of Nuclear Physics of the Ministry of Energy of the Republic of Kazakhstan, 1 Ibragimov Street, 050032, Almaty, Kazakhstan
[‡] also at: SNOLAB, Creighton Mine #9, 1039 Regional Road 24, Sudbury, ON P3Y 1N2, Canada
[§] also at: Lebedev Physical Institute of the Russian Academy of Sciences, 53 Leninskiy Prospect, 119991, Moscow, Russia